Topological Characterization of HXO 2 (X = Cl, Br, I) Isomerization

ARTICLE *in* THE JOURNAL OF PHYSICAL CHEMISTRY A · MARCH 2007

Impact Factor: 2.69 · DOI: 10.1021/jp067526b · Source: PubMed

Topological Characterization of HXO_2 (X = Cl, Br, I) Isomerization

Xiaoyan Li,[†,‡] Yanli Zeng,[†] Lingpeng Meng,[†] and Shijun Zheng*[,†]

Institute of Computational Quantum Chemistry, College of Chemistry, Hebei Normal University, Yuhua Road, Shijiazhuang, 050016, China, and Department of Chemistry, Graduate School, Chinese Academy of Sciences, Beijing 100049, China

Received: November 14, 2006; In Final Form: December 29, 2006

The isomerization reactions of HOOX → HOXO → HXO_2 (X = Cl, Br, I) have been studied by using the density functional theory. The breakage and formation of the chemical bonds of the titled reactions have been discussed by the topological analysis method of electronic density. The calculated results show that there is a transitional structure of a three-membered ring on each of the isomerization reaction paths. The "energy transition state (ETS)" and the "structure transition state (STS)" in all of the studied reactions have been found. In all these reactions, the position of the structure transition state and the scope of the structure transition region correlate well with the reaction energy. The STS appears after the ETS in the exothermic reaction but it appears before the ETS in the endothermic reaction. The less reaction energy there is, the wider scope of the structure transition region.

1. Introduction

Stratospheric ozone abundance is largely determined by the rate of the catalytic chain processes which destroy ozone and by the concentration of the chain carriers and their precursors. Among various species, the radical carriers of HO_x ($x = 1, 2$), ClO_x ($x = 0, 1$), BrO_x ($x = 0, 1$), and IO_x ($x = 0, 1$) families have been identified as the major species in determining the ozone concentration in the Earth's atmosphere.[1−6] The reactions between XO (X = Cl, Br, I) and OH are crucial as their interaction could lead to either another chain carrier (chain transfer) or a reservoir molecule. There have been some ab initio and DFT studies performed on the isomers of HXO_2 (X = Cl, Br) which suggest that HOOX (X = Cl, Br) is the lowest energy structure of all the HXO_2 (X = Cl, Br) isomers.[7−10]

To our knowledge, the topological structures of these reactions have not yet been included in any of these studies. Obtaining an understanding of HXO_2 (X = Cl, Br, I) isomers and their topological properties is very desirable; however, as we know, judging the breaking or formation of a bond is almost impossible with experimental methods and the traditional population analysis. According to the theory of "atoms in molecules (AIM)",[11−15] topological studies on reaction paths of some typical reactions have been carried out by some authors in recent years,[11−17] but much more is still to be known about the relationship between topological characteristics of density distribution and the energy variation along the reaction path.

In this paper, we carried out studies on the reactions of HOOX → HOXO → HXO_2 (X = Cl, Br, I), trying to give a clear picture for topological characteristics of these reactions. The breakage and formation of the bonds in the isomerization reaction paths have been discussed; the structure transition state and the structure transition region of the titled reaction are found. It is noted that the goal of this work is not to discuss the isomerization mechanism. Instead, we are pursuing the systematic relationship between topological characteristic of density distribution and the energy variations along the reaction paths. This paper is an extension and an additional example of the established ideas and concepts of AIM.[11−15]

2. Computational Methods

The geometries of reactants, transition states, and products on the potential energy surface were located by B3LYP calculations. The 6-311++G(d, p) basis set was used for H, O, Cl, and Br, and the basis sets used for element I was taken from ref 18. The *d* polar functions were split into $\alpha_1(d_{polar}) = 0.604$ and $\alpha_2(d_{polar}) = 0.151$ by us. The reaction paths have been traced out by Intrinsic Reaction Coordinate (IRC)[19] in mass-weighted internal coordinates going in forward and reverse directions from the transition state with the step size equal to 0.01 $(amu)^{1/2}$·b. The energies of these compound were corrected at MP2(Full)/6-311++G(d, p) and CCSD/6-311++G(2d, 2p) level. The calculations were made using the Gaussian 98 program.[20] Topological analyses were carried out with program AIM 2000.[21] Maps of the gradient vector field of electron density of HOOX → HOXO → HXO_2 (X = Cl, Br, and I, Figures 3−5), which are based on B3LYP/6-311++G(2d, 2p) calculations, were plotted by program AIM 2000.[21]

3. Results and Discussion

3.1. Potential Energy Curves on IRC Paths. Computations on the isomeric forms, HOOX, HOXO, and HXO_2 (X = Cl, Br), were previously performed by some groups using different methods.[7−10] We have re-examined these geometries using B3LYP/6-311++G(d, p). Our calculated structure of HXO_2 (X = Cl, Br) isomers agree very well with those reported.[7−10] This suggests that the results obtained from the B3LYP/6-311++G-(d, p) is quite reasonable. The calculated geometries of HIO_2 isomers are similar to those of HXO_2 (X = Cl, Br) isomers.

* Corresponding author. Tel./fax: +86 311 86269217. E-mail: sjzheng@mail.hebtu.edu.cn.
† Hebei Normal University.
‡ Chinese Academy of Sciences.

10.1021/jp067526b CCC: $37.00
Published on Web 02/03/2007

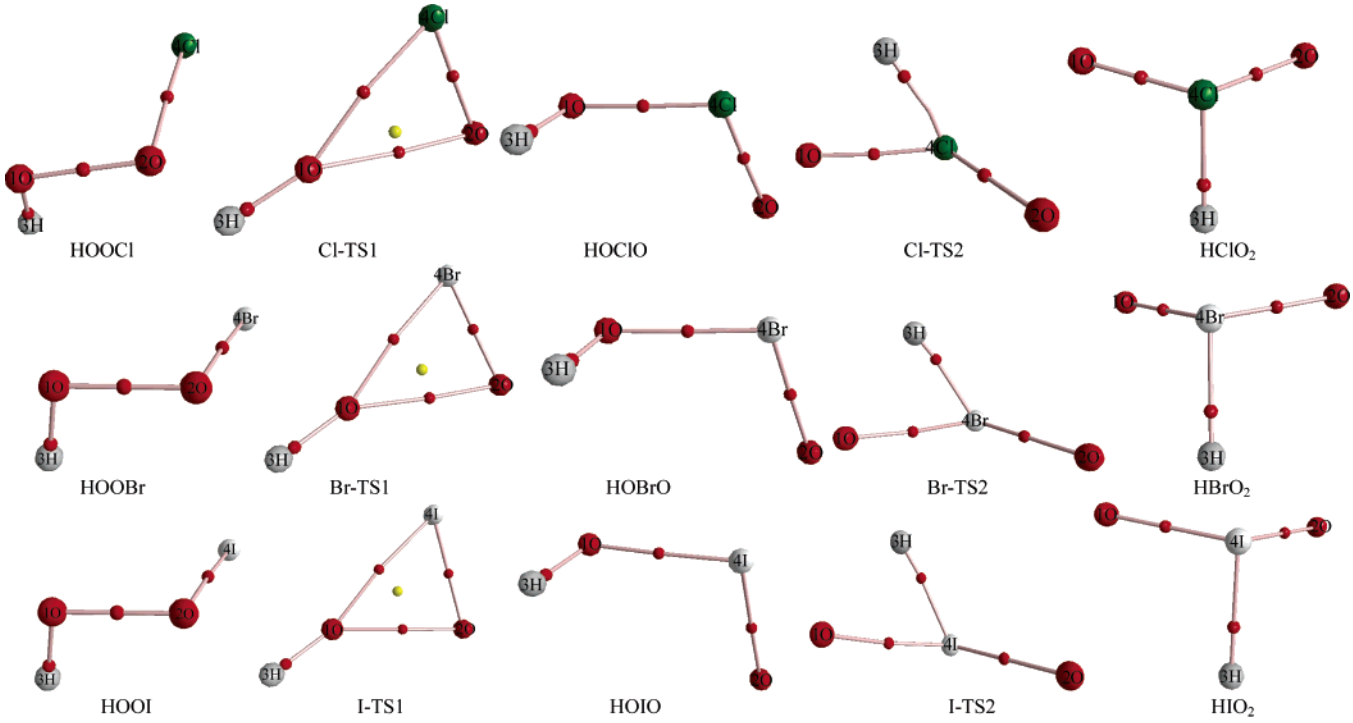

Figure 1. Molecular graph of reactants, transition states, and products.

The geometry parameters of the reactants, transition states, intermediates, and products on the potential energy surfaces have been optimized and shown in Figure 1s of the Supporting Information. The 3D molecular graphs of these compounds are plotted in Figure 1. The vibrating frequencies were computed for the stationary point characterization and zero-point energy (ZPE) corrections were included. IRC calculations were carried out to validate the connection of the reactant, transition states, and products. The potential energy curves of the titled reactions are shown in Figure 2. The absolute energies, ZPE values, relative energies, thermal enthalpies, and Gibbs free energies are listed in Table 1s of the Supporting Information. CCSD-(T)/6-311++G(2d, 2p) energies are to be used in the following discussion.

As shown in Figure 2 and Table 1s, in HXO_2 (X = Cl, Br) isomers, the energy of HOOX (X = Cl, Br) is the lowest and the next is HOXO; the energy of HXO_2 is the highest and it is thus the least stable. The relative energies of HOClO to HOOCl and HOBrO to HOOBr are 14.8 and 9.4 kcal/mol, respectively. The energies of $HClO_2$ and $HBrO_2$ are 67.7 and 66.0 kcal/mol higher than that of HOOCl and HOOBr. For the HOOX (X = Cl, Br) → HOXO (X = Cl, Br) reaction, the energy barriers are 43.6 and 42.2 kcal/mol. For the HOXO (X = Cl, Br) → HXO_2 (X = Cl, Br) process, the energy barriers were found to be 89.8 and 88.5 kcal/mol. The energy barrier is too high to allow the interconversion of HOXO (X = Cl, Br) → HXO_2 (X = Cl, Br). In HIO_2 isomers, the relative stability of the three isomers is of the order HOIO < HOOI < HIO_2. HOIO is 18.2 and 31.7 kcal/mol lower in energy than HOOI and HIO_2. The barrier height of HOOI → HOIO and HOIO → HXO_2 is 28.6 and 47.4 kcal/mol, respectively. So HOOI and HOIO could convert to each other and HOIO could transform to HIO_2.

3.2. Topological Analyses of Electronic Density on IRC Paths. For each reaction, the topological analysis was carried out on the electronic density of some points along the reaction path. Topological properties of HOOX → HOXO → HXO_2 (X = Cl, Br and I) are listed in Tables 1−3, respectively. Gradient vector field of the electronic density are plotted for some points along the reaction path and displayed in Figures 3−5 for HOOX → HOXO → HXO_2 (X = Cl, Br, I), respectively.

3.2.1. Changes in Structure Determined by the Topology of the Electron Density. According to the topological analysis of electronic density in the theory of AIM,[22,23] electron density $\rho(r_c)$ is used to describe the strength of a bond and Laplacian of the electron density ($\nabla^2\rho(r_c)$) describes the characteristics of the bond. The Laplacian $\nabla^2\rho(r_c)$ is the sum of λ_1, λ_2 and λ_3, λ_i is one of the eigenvalues of the Hessian matrix of electronic density. If a critical point has two negative and one positive eigenvalue, it is called (3, −1) saddle point or the Bond critical Point (BCP). If a critical point has two positive and one negative eigenvalues, it is called (3, +1) critical point or the Ring Critical Point (RCP); the (3, +1) critical point is characteristic of a ring structural region. We assign S1a, S2a, S3a, S1b, S2b, and S3b as reaction coordinates for processes of HOOX → HOXO (X = Cl, Br, I) and HOXO → HXO_2 (X = Cl, Br, I), respectively.

In the HOOX → HOXO (X = Cl, Br, I) process, the electronic density $\rho(r_c)$ at the BCP of the O−O bond becomes smaller and smaller, which indicates that the O−O bond becomes weaker and weaker, and at last is broken. As the reactions proceed, the $\rho(r_c)$ at the BCP of X−O1 (X = Cl, Br, I) bond become larger and larger, which indicates that the X−O1 (X = Cl, Br, I) bonds become stronger and stronger, and then HOXO (X = Cl, Br, I) comes into being. As the reaction proceeds, the $\rho(r_c)$ of the BCP of the X−O2 (X = Cl, Br, I) bond becomes somewhat larger, which indicates that the X−O2 (X = Cl, Br, I) bond becomes somewhat stronger.

In the HOXO → HXO_2 (X = Cl, Br, and I) process, the electronic density $\rho(r_c)$ at the bond of H−O1 becomes smaller and smaller, which indicates that the H−O1 bond becomes weaker and weaker, and at last is broken. As the reactions proceed, the H−X (X = Cl, Br, I) bonds become larger and larger, which indicates that the H−X (X = Cl, Br, I) bonds become stronger and stronger, and then HXO_2 (X = Cl, Br, I) forms.

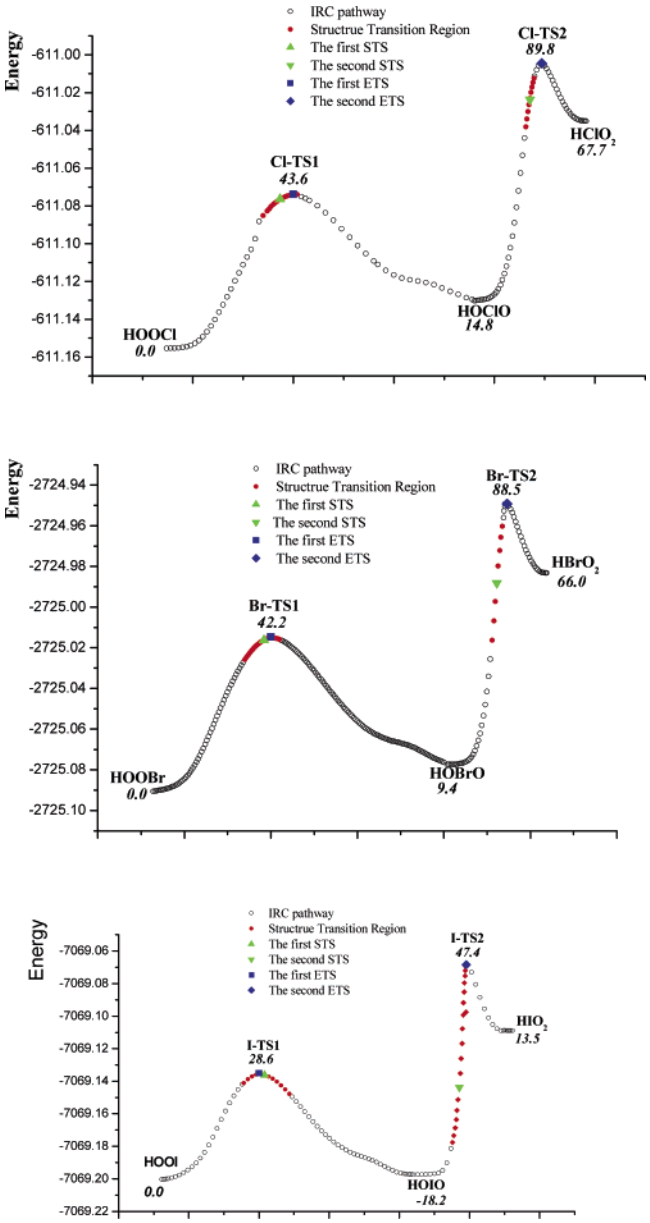

Figure 2. Potential energy curves of reaction HOOX → HOXO → HXO_2 (X = Cl, Br, I). (The italic numbers are relative energy (kcal/mol) at CCSD/6-311++G(2d, 2p) level.)

TABLE 1: Topological Properties at BCP and RCP of the Ring Structure Transition Region the Given Reaciton

			eigenvalues of the Hessian matrix			
	$S/(amu)^{1/2}\cdot b$	ρ	λ_1	λ_2	λ_3	$\nabla^2\rho$
		HOOCl → HOClO				
RCP	S1a = −1.32	0.0434	−0.0450	0.0068	0.2835	0.2453
	S1a = −0.66	0.0433	−0.0466	0.0329	0.2714	0.2577
	S1a = −0.65 (STS)	0.0433	−0.0473	0.0330	0.2852	0.2709
	S1a = −0.64	0.0432	−0.0465	0.0329	0.2715	0.2579
	ETS	0.0409	−0.0450	0.0082	0.2900	0.2532
	S1a = +0.02	0.0407	−0.0452	0.0022	0.2965	0.2535
Cl−O_1	S1a = −1.32	0.0434	−0.0447	−0.0065	0.2903	0.2391
	S1a = −0.65	0.0464	−0.0487	−0.0328	0.3208	0.2393
	ETS (S1a = 0.0)	0.0526	−0.0567	−0.0508	0.3240	0.2165
	S1a = +0.02	0.0528	−0.0570	−0.0513	0.3246	0.2163
	HOClO	0.1698	−0.2687	−0.2543	0.6449	0.1219
O−O	HOOCl	0.3161	−0.7400	−0.7315	1.5704	0.0989
	S1a = −1.32	0.0578	−0.0749	−0.0688	0.3916	0.2479
	S1a = −0.65	0.0510	−0.0624	−0.0499	0.3333	0.2210
	ETS (S1a = 0.0)	0.0409	−0.0458	−0.0081	0.3006	0.2467
	S1a = +0.02	0.0407	−0.0452	−0.0022	0.2965	0.2491
Cl−O_2	HOOCl	0.1584	−0.2456	−0.2257	0.5715	0.1002
	S1a = −1.32	0.2580	−0.4222	−0.4195	0.6117	−0.2300
	S1a = −0.65	0.2650	−0.4376	−0.4331	0.6200	−0.2507
	ETS (S1a = 0.0)	0.2706	−0.4498	−0.4443	0.6318	−0.2623
	S1a = +0.02	0.2708	−0.4502	−0.4447	0.6322	−0.2627
	HOClO	0.2829	−0.4726	−0.4639	0.7096	−0.2269
		HOC1O → $HC1O_2$				
RCP	S1b = −0.83	0.1386	−0.2754	0.0357	0.3952	0.1555
	S1b = −0.63	0.1374	−0.2490	0.2236	0.2785	0.2531
	S1b = −0.62 (STS)	0.1373	−0.2485	0.2259	0.2774	0.2548
	S1b = −0.61	0.1371	−0.2480	0.2255	0.2779	0.2554
	S1b = −0.43	0.1285	−0.2622	0.0065	0.4560	0.2003
H−O	HOClO	0.3684	−1.8286	−1.7789	0.9168	−2.6907
	S1b = −0.83	0.1865	−0.5414	−0.4675	0.7121	−0.2968
	S1b = −0.62	0.1523	−0.3696	−0.2556	0.5678	−0.0574
	S1b = −0.43	0.1865	−0.2622	−0.0067	0.4558	0.1869
Cl−O	HOClO	0.1698	−0.2687	−0.2543	0.6449	0.1219
	S1b = −0.83	0.2031	−0.3495	−0.3101	0.7106	0.0510
	S1b = −0.62	0.2034	−0.3225	−0.3048	0.7111	0.0838
	S1b = −0.43	0.2066	−0.3531	−0.3341	0.7270	0.0398
	ETS (S1b = 0.0)	0.2099	−0.3342	−0.3218	0.7410	0.0850
	$HclO_2$	0.3076	−0.5359	−0.5318	0.7481	−0.3196
H−Cl	S1b = −0.83	0.1386	−0.2818	−0.0351	0.4154	0.0985
	S1b = −0.62	0.1494	−0.3280	−0.2159	0.4446	−0.0993
	S1b = −0.43	0.1685	−0.4101	−0.3447	0.4815	−0.2733
	ETS (S1b = 0.0)	0.2018	−0.5161	−0.4787	0.5010	−0.4938
	$HClO_2$	0.2180	−0.5354	−0.5223	0.5319	−0.5258

For the reaction of HOOCl → HOClO, from the reactant HOOCl to S1a = −1.33, the O−O bond becomes weaker and weaker and the bond path becomes more and more bent. At S1a = −1.32, Cl is bonded to atom O1, a new bond Cl−O1 has been formed, but the Cl−O2 bond still exists at this time. Therefore, Cl, O1, and O2 form a ring structure; a RCP appears. As the RCP just appears, it is very close to the BCP of Cl−O1. As the process proceeds, RCP moves to the center of the ring. The λ_2 of the Hessian matrix at RCP increases and reaches the maximum at S1a = −0.65. After this point the λ_2 decreases gradually. The point of S1a = +0.65 is the so-called STS in the reaction. At the point S1a = +0.03, the Cl−O2 bond has been broken and the RCP disappeared. And then the Cl−O1 bond becomes stronger and stronger, and the product HOClO forms. For the reaction of HOClO → $HClO_2$, at S1b = −0.83, H is bonded to atom O1, a new bond H−O1 has been formed, and the Cl−H bond still exists at this time. Therefore, O1, H, and Cl form a ring structure, a RCP appears, and it exits in the region of S1b = −0.83 to S1b = −0.43. S1b = −0.62 is the STS of the reaction as is shown in Table 1.

The HOOBr → HOBrO → $HBrO_2$ and HOOI → HOIO → HIO_2 processes are similar to the HOOCl → HOClO → $HClO_2$ process: There is a bifurcation-type X−O1−O2 (X = Br, I) and H−O1−X (X = Br, I) ring structure that appears in the HOOX → HOXO (X = Br, I) and HOXO → HXO_2 (X = Br, I) processes, respectively. (As shown in Tables 2 and 3, the RCP exists in Br−O1−O2, S2a = −1.25 → S2a = +0.60; H−O1−Br, S2b = −0.85 → S2b = −0.33; I−O1−O2, S3a = −1.11 → S3a = +1.85; H−O1−I: S3b = −0.88 → *S*2b = −0.12).

3.2.2. Structure Transition State and Structure Transition Region. When an old bond broke and a new bond formed, the "structure transition state (STS)" and "structure transition region" appeared.[22,23] There are two kinds of STSs: one of them is ring structure transition. As the RCP just appears, RCP is very close to the BCP of a newly formed bond. As the process

TABLE 2: Topological Properties at BCP and RCP of the Ring Structure Transition Region for the Given Reaction

			eigenvalues of the Hessian matrix $\nabla^2\rho$			
	S/(amu)$^{1/2}$·b	ρ	λ_1	λ_2	λ_3	$\nabla^2\rho$
		HOOBr → HOBrO				
RCP	S2a = −1.25	0.0421	−0.0397	0.0027	0.2572	0.2202
	S2a = −0.28	0.0419	−0.0417	0.0377	0.2402	0.2362
	S2a = −0.27 (STS)	0.0418	−0.0417	0.0378	0.2404	0.2365
	S2a = −0.26	0.0418	−0.0416	0.0378	0.2404	0.2366
	ETS (S2a = −0.00)	0.0412	−0.0413	0.0361	0.2431	0.2379
	S2a = 0.60	0.0384	−0.0393	0.0063	0.2671	0.2341
Br−O_1	S2a = −1.25	0.0421	−0.0396	−0.0026	0.2597	0.2175
	S2a = −0.27	0.0468	−0.0447	−0.0358	0.2754	0.1949
	ETS (S2a = 0.0)	0.0485	−0.0469	−0.0405	0.2778	0.1904
	S2a = 0.60	0.0542	−0.0539	−0.0528	0.2889	0.1822
	HOBrO	0.1433	−0.2043	−0.1925	0.5287	0.1319
O−O	HOOBr	0.3088	−0.7155	−0.7073	1.5314	0.1086
	S2a = −1.25	0.0644	−0.0850	−0.0844	0.4265	0.2571
	S2a = −0.27	0.0487	−0.0574	−0.0477	0.3470	0.2419
	ETS (S2a = 0.0)	0.0454	−0.0518	−0.0039	0.3290	0.2733
	S2a = 0.60	0.0384	−0.0400	−0.0062	0.2776	0.2314
Br−O_2	HOOBr	0.1303	−0.1808	−0.1670	0.4640	0.1162
	S2a = −1.25	0.2033	−0.3011	−0.3003	0.6749	0.0735
	S2a = −0.27	0.2105	−0.3129	−0.3125	0.6802	0.0548
	ETS (S2a = 0.0)	0.2118	−0.3151	−0.3146	0.6798	0.0501
	S2a = 0.60	0.2154	−0.3210	−0.3203	0.6808	0.0395
	HOBrO	0.2217	−0.3268	−0.3242	0.6770	0.0260
		HOBrO → $HBrO_2$				
RCP	S2b = −0.85	0.1168	−0.1935	0.0325	0.3238	0.1628
	S2b = −0.62	0.1163	−0.1855	0.1915	0.2424	0.2484
	S2b = −0.61 (STS)	0.1161	−0.1852	0.1922	0.2418	0.2488
	S2b = −0.60	0.1208	−0.2042	0.1612	0.1898	0.1468
	S2b = −0.33	0.1052	−0.1762	0.0145	0.3702	0.2085
H−O	HOBrO	0.3663	−1.7986	−1.7549	0.9029	−2.6506
	S2b = −0.85	0.1733	−0.4646	−0.4210	0.6166	−0.2690
	S2b = −0.61	0.1354	−0.3013	−0.2316	0.5018	−0.0311
	S2b = −0.33	0.1052	−0.1802	−0.0144	0.3843	0.1897
Br−O	HOBrO	0.1433	−0.2043	−0.1925	0.5287	0.1319
	S2b = −0.85	0.1666	−0.2382	−0.2173	0.5794	0.1239
	S2b = −0.61	0.1677	−0.2381	−0.2238	0.5731	0.1112
	S2b = −0.33	0.1692	−0.2391	−0.2317	0.5685	0.0977
	ETS (S2b = 0.00)	0.1717	−0.2442	−0.2359	0.5682	0.0881
	$HBrO_2$	0.2071	−0.3061	−0.3581	0.7234	0.0592
H−Br	S2b = −0.85	0.1168	−0.1992	−0.0312	0.3351	0.1047
	S2b = −0.61	0.1298	−0.2449	−0.1738	0.3351	−0.0836
	S2b = −0.33	0.1475	−0.2949	−0.2537	0.3366	−0.2120
	ETS (S2b = 0.00)	0.1664	−0.3436	−0.3181	0.3438	−0.3179
	$HBrO_2$	0.1760	−0.3504	−0.3419	0.3592	−0.3331

TABLE 3: Topological Properties at BCP and RCP of the Ring Structure Transition Region for the Given Reaction

			eigenvalues of the Hessian matrix			
	S/(amu)$^{1/2}$·b	ρ	λ_1	λ_2	λ_3	$\nabla^2\rho$
		HOOI → HOIO				
RCP	S3a = −1.11	0.0423	−0.0388	0.0045	0.2348	0.2005
	ETS (S3a = 0.0)	0.0429	−0.0417	0.0426	0.2153	0.2162
	S3a = +0.35	0.0425	−0.0415	0.0443	0.2167	0.2195
	S3a = +0.36 (STS)	0.0425	−0.0415	0.0443	0.2166	0.2194
	S3a = +0.37	0.0424	−0.0415	0.0443	0.2169	0.2197
	S3a = +1.85	0.0378	−0.0373	0.0057	0.2509	0.2193
I−O_1	S3a = −1.11	0.0423	−0.0384	−0.0043	0.2399	0.1972
	ETS (S3a = 0.0)	0.0476	−0.0441	−0.0356	0.2606	0.1809
	S3a = +0.36	0.0494	−0.0462	−0.0405	0.2640	0.1773
	S3a = +1.85	0.0610	−0.0649	−0.0618	0.2920	0.1653
	HOIO	0.1191	−0.1602	−0.1525	0.5736	0.2609
O−O	HOOI	0.2920	−0.6693	−0.6490	1.4382	0.1199
	S3a = −1.11	0.0750	−0.1022	−0.1005	0.4902	0.2875
	ETS (S3a = 0.0)	0.0550	−0.0664	−0.0616	0.3910	0.263
	S3a = 0.36	0.0521	−0.0598	−0.0533	0.3693	0.2562
	S3a = 1.85	0.0378	−0.0376	−0.0055	0.2606	0.2175
I−O_2	HOOI	0.1115	−0.1473	−0.1391	0.5074	0.221
	S3a = −1.11	0.01558	−0.2226	−0.2203	0.8403	0.3974
	ETS (S3a = 0.0)	0.1622	−0.2326	−0.2299	0.8447	0.3822
	S3a = 0.36	0.1630	−0.2336	−0.2307	0.8368	0.3725
	S3a = 1.85	0.1677	−0.2400	−0.2362	0.8165	0.3403
	HOIO	0.1728	−0.2418	−0.2406	0.7861	0.3037
		HOIO → HIO_2				
RCP	S3b = −0.88	0.1050	−0.1504	0.0258	0.2882	0.1636
	S3b = −0.53	0.1047	−0.1460	0.1457	0.2385	0.2382
	S3b = −0.52 (STS)	0.1046	−0.1458	0.1457	0.2383	0.2382
	S3b = −0.51	0.1044	−0.1456	0.1456	0.2383	0.2383
	S3b = −0.12	0.0923	−0.1345	0.0237	0.3273	0.2165
H−O	HOIO	0.3677	−1.8104	−1.7724	0.9136	−2.6692
	S3b = −0.88	0.1893	−0.5098	−0.4792	0.6492	−0.3398
	S3b = −0.52	0.1306	−0.2644	−0.2127	0.4751	−0.0020
	S3b = −0.12	0.0923	−0.1405	−0.0236	0.3563	0.1922
I−O	HOIO	0.1191	−0.1602	−0.1525	0.5736	0.2609
	S3b = −0.88	0.1323	−0.1799	−0.1483	0.6253	0.2971
	S3b = −0.52	0.1333	−0.1800	−0.1579	0.5979	0.2600
	S3b = −0.12	0.1354	−0.1812	−0.1724	0.5688	0.2152
	ETS (S = 0.0)	0.1362	−0.1818	−0.1763	0.5623	0.2042
	S3b = −0.51	0.1044	−0.1456	0.1456	0.2383	0.2383
	S3b = −0.12	0.0923	−0.1345	0.0237	0.3273	0.2165
H−O	HOIO	0.3677	−1.8104	−1.7724	0.9136	−2.6692
	S3b = −0.88	0.1893	−0.5098	−0.4792	0.6492	−0.3398
	S3b = −0.52	0.1306	−0.2644	−0.2127	0.4751	−0.0020
	S3b = −0.12	0.0923	−0.1405	−0.0236	0.3563	0.1922
I−O	HOIO	0.1191	−0.1602	−0.1525	0.5736	0.2609
	S3b = −0.88	0.1323	−0.1799	−0.1483	0.6253	0.2971
	S3b = −0.52	0.1333	−0.1800	−0.1579	0.5979	0.2600
	S3b = −0.12	0.1354	−0.1812	−0.1724	0.5688	0.2152
	ETS (S = 0.0)	0.1362	−0.1818	−0.1763	0.5623	0.2042
	HIO_2	0.1822	−0.2611	−0.2568	0.8449	0.3270
H−I	S3b = −0.88	0.1051	−0.1536	−0.0252	0.2872	0.1084
	S3b = −0.51	0.1236	−0.1969	−0.1554	0.2646	−0.0877
	S3b = −0.12	0.1443	−0.2372	−0.2170	0.2757	−0.1785
	HIO_2	0.1600	−0.2614	−0.2536	0.3861	−0.1289

proceeds, RCP moves to the center of the ring. When the RCP goes to the BCP of another bond, this bond is broken and the ring disappears. From the ring's appearance to its disappearance called "structure transition regions", the λ_2 eigenvalue of the Hessian matrix of the RCP (the positive curvature lying in the plane) has the trend of zero → maximum → zero. We call the maximum Hessian matrix λ_2 of the RCP as STS and the traditional transition state that is the maximum on the energy surface as "energy transition state (ETS)".

In the isomerization reactions of HOOX → HOXO → HXO_2 (X = Cl, Br, I), the ring structure transition region appears. The regions of S1a = −1.32 → S1a = +0.02 for the HOOCl → HOClO process, S1b = −0.83 → S1b = −0.43 for the HOClO → $HClO_2$ process, S2a = −1.25 → S2a = +0.60 for the HOOBr → HOBrO process, S2b = −0.85 → S2b = −0.33 for the HOBrO → $HBrO_2$ process, S3a = −1.11 → S3a = +1.85 for the HOOI → HOIO process, and S3b = −0.88 → S2b = −0.12 for the HOIO → HIO_2 process, respectively. The three-membered ring STSs of the structure transition regions are S1a = −0.65, S1b = −0.62, S2a = −0.27, S2b = −0.61, S3a = +0.36, and S3b = −0.52.

Figure 2 also gives the position of the STS, ETS, and transition state region along the reaction pathways. The position of STS is not the position of ETS. In endothermic reactions (HOOCl → HOClO → $HClO_2$, HOOBr → HOBrO → $HBrO_2$, HOIO → HIO_2), the STS appears before the ETS. It appears earlier and earlier, in relation to the ETS, according to the reaction energy. But in the exothermic reaction (HOOI → HOIO), the STS appears after the ETS. Furthermore, the more the reaction energy absorbs, the earlier the STS appears.

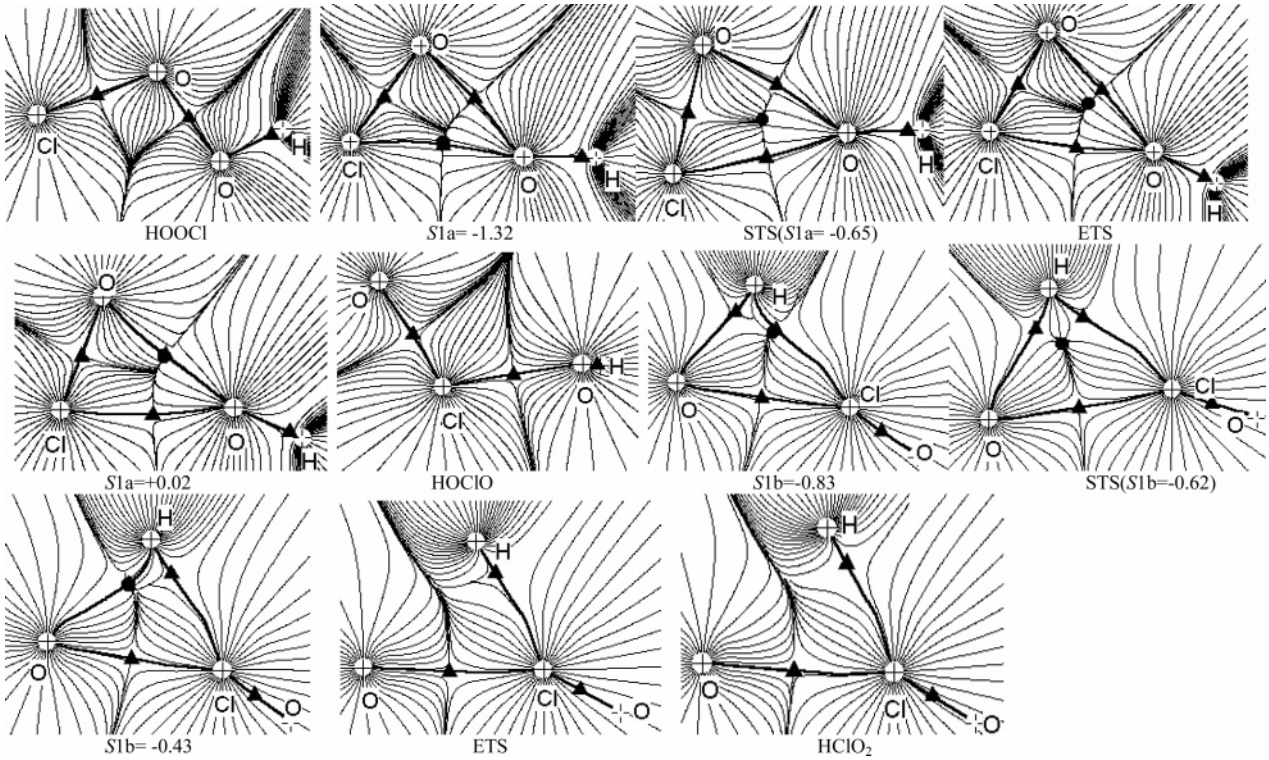

Figure 3. Maps of gradient vector field of electron density of isomerization reaction of $HClO_2$ (+ represents nuclear of atomic; ▲ represents bond critical point; ● represents ring critical point).

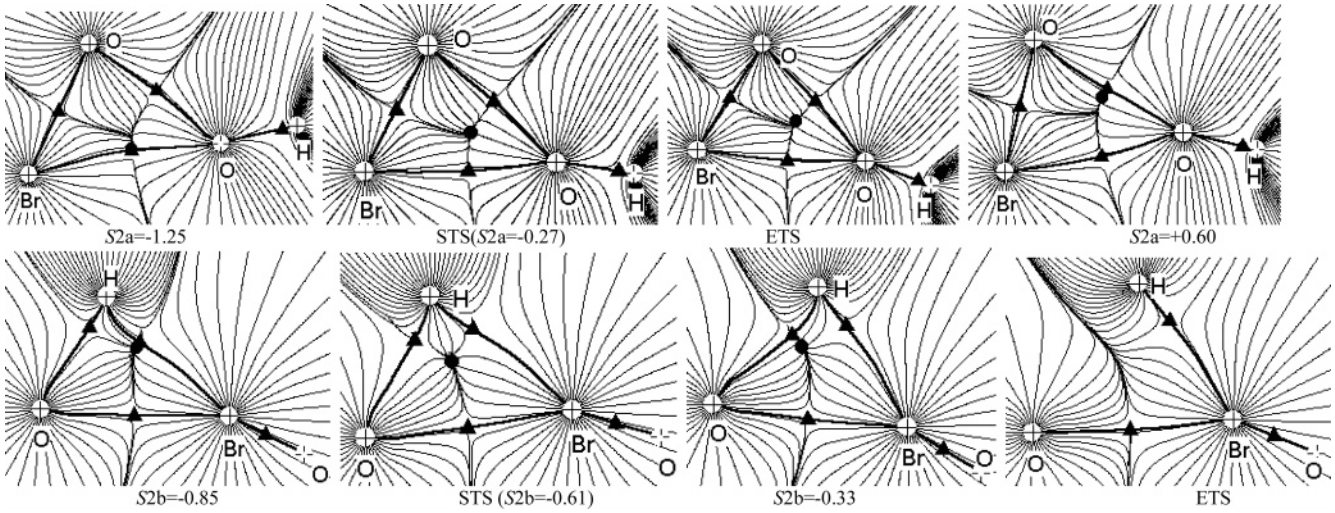

Figure 4. Maps of gradient vector field of electron density of isomerization reaction of $HBrO_2$ (+ represents nuclear of atomic; ▲ represents bond critical point; ● represents ring critical point).

TABLE 4. Reaction Energy and Scope of Structure Transition Region of the Isomerization Reaction of HOOX → HOXO → HXO_2 (X = Cl, Br, I)

	energy (kcal/mol)	scope of structure transition region		energy (kcal/mol)	scope of structure transition region
HOOCl−HOClO	14.8	1.34 ($S = -1.32 \rightarrow +0.02$)	HOClO−$HClO_2$	52.9	0.40 ($S = -0.83 \rightarrow -0.43$)
HOOBr−HOBrO	9.4	1.85 ($S = -1.25 \rightarrow +0.60$)	HOBrO−$HBrO_2$	56.6	0.52 ($S = -0.85 \rightarrow -0.33$)
HOOI−HOIO	18.2	2.96 ($S = -1.11 \rightarrow +1.85$)	HOIO−HIO_2	31.7	0.76 ($S = -0.88 \rightarrow -0.12$)

Furthermore, as shown in Figures 2−5, the structure transition region becomes wider and wider in the sequence of Cl, Br, and I. From Figure 2 and Tables 1−3, Table 4 is concluded. For the HOOCl−HOClO process, the reaction energy is 14.8 kcal/mol, and the scope of the structure transition region of the process is S1a = $-1.32 \rightarrow +0.02$. The reaction energy of the HOClO−$HClO_2$ process is 52.9 kcal/mol and the scope of the structure transition region of the process is S1b = $-0.83 \rightarrow -0.43$. The reaction energy of HOOCl−HOClO is lower than that of the HOClO−$HClO_2$ process; the scope of the structure

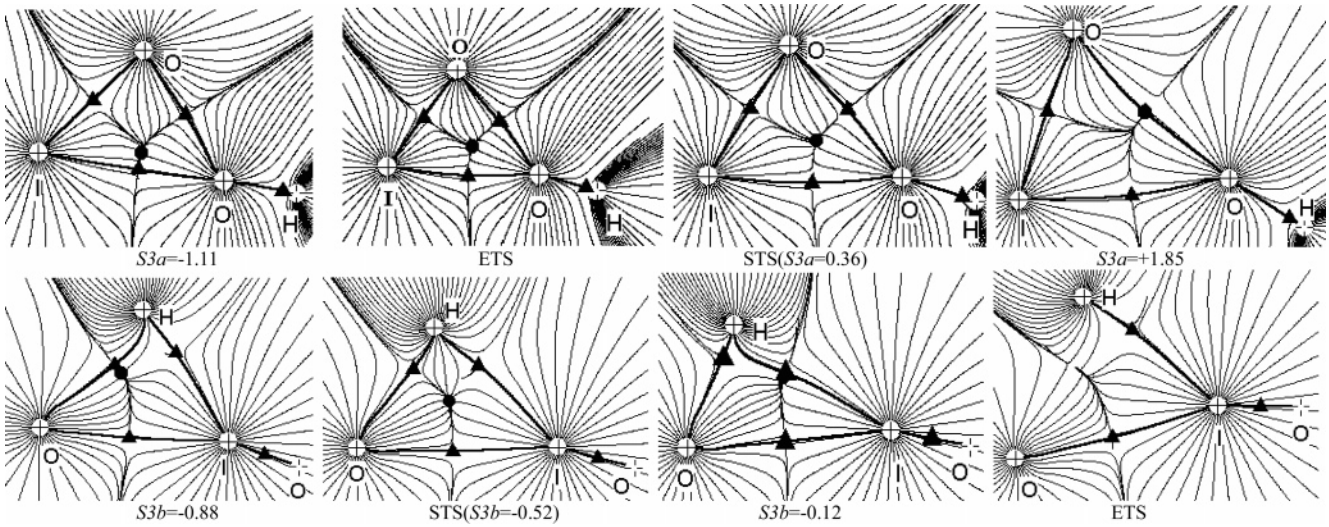

Figure 5. Maps of gradient vector field of electron density of isomerization reaction of HIO_2 (+ represents nuclear of atomic; ▲ represents bond critical point; ● represents ring critical point).

transition region of HOOCl−HOClO is wider than that of the HOClO−$HClO_2$ process. This trend can be applied to HOOX−HOXO and HOXO−HXO_2 (X = Br, I) processes. Therefore, the less the reaction energy, the wider the scope of the structure transition region.

The scope of the structure transition region of HOOCl−HOClO, HOOBr−HOBrO, and HOOI−HOIO are S1a = −1.32 → +0.02, S1b = −1.25 → +0.60, and S1c = −1.11 → +1.85, respectively. The scope of the structure transition region of HOClO−$HClO_2$, HOBrO−$HBrO_2$, and HOIO−HIO_2 are S2a = −0.83 → −0.43, S2b = −0.85 → −0.33, and S2c = −0.88 → −0.12, respectively. The structure transition region becomes wider and wider in the sequence of Cl, Br, and I. The increased van der Waals and covalent radii of Cl, Br, and I can explain the sequence of the width of the ring structure transition regions.

4. Conclusions

(1) The breakage and formation of the chemical bonds in the reactions have been discussed by the topological analysis method of electronic density.

(2) There is a transitional structure of three-membered ring on the isomerization reaction paths.

(3) In all these reactions, the position of the structure transition state and the scope of the structure transition region correlate well with the reaction energy. The STS appears after the ETS in exothermic reaction but it appears before the ETS in endothermic reaction. The less the reaction energy, the wider the scope of the structure transition region.

Acknowledgment. This project was supported by the National Natural Science Foundation of China (Contract No. 20573032, 20503035) and the Natural Science Foundation of Hebei Province (Contract No. B2006000137, B2006000131). Li Xiaoyan would like to thank the Chinese Academy of Sciences for a scholarship for the period of this work.

Supporting Information Available: Energies (E), Enthalpies (H), and Gibbs Free Energy (G) for the various compounds at MP2/6-311++G(d, p) and CCSD/6-311++G(2d,2p) levels are tabulated in Table 1S. Geometries of reactants, transition states, and products are shown in Figure 1S. This material is available free of charge via the Internet at http://pubs.acs.org.

References and Notes

(1) Molina, M. J.; Rowland, F. S. *Nature* **1974**, *249*, 810.
(2) Wayne, R. P.; Poulet, G.; Biggs, P.; Burrows, J. P.; Cox, R. A.; Crutzen, P. J.; Hayman, G. D.; Jenkin, M. E.; Le Bras, G.; Mortgat, G. K.; Platt, U.; Schinderler, R. N. *Atmos. Environ.* **1995**, *29*, 2677.
(3) Barrett, J. W.; Solomon, P. N.; de Zafra, R. L.; Jaramillo, M.; Emmons, L.; Parrish, A. *Nature* **1988**, *336*, 455.
(4) Anderson, J. G.; Toohey, D. W.; Brune, W. H. *Science* **1991**, *251*, 39.
(5) Wennberg, P. O.; Cohen, R. C.; Stimpfle, R. M.; Koplow, J. P.; Anderson, J. G.; Salawitch, R. J.; Fahey, D. W.; Woodbridge, E. L.; Keim, E. R.; Gao, R. S.; Webster, C. R.; May, R. D.; Toohey, D. W.; Avallone, L. M.; Proffitt, M. H.; Loewenstein, M.; Podolske, J. R.; Chan, K. R.; Wofsy, S. C. *Science* **1994**, *226*, 398.
(6) Solomon, S.; Garcia, R. R.; Ravishankara, A. R. *J. Geophys. Res.* **1994**, *99*, 20491.
(7) Francisco, J. S.; Sander, S. P.; Lee, T. J.; Rendell, A. P. *J. Phys. Chem.* **1994**, *98*, 5644.
(8) Sumathi, R.; Peyerímhoff, S. D. *J. Phys. Chem. A* **1999**, *103*, 7515.
(9) Guha, S.; Francisco, J. S. *Chem. Phys.* **1999**, *247*, 387.
(10) Timothy, L. J. *Chem. Phys. Lett.* **1996**, *262*, 559.
(11) Bader, R. F. W.; Nguyen-Dang, T. T.; Tal, Y. *J. Chem. Phys.* **1979**, *70*, 4316.
(12) Tal, Y.; Bader, R. F. W.; Nguyen-Dang, T. T. *J. Chem. Phys.* **1981**, *74*, 5162.
(13) Bader, R. F. W.; Nguyen-Dang, T. T.; Tal, Y. *Pep. Prog. Phys.* **1981**, *44*, 893.
(14) Bader, R. F. W. *Atoms in Molecules: A Quantum Theory*; Clarendon Press: Oxford, U. K., 1990.
(15) Bader, R. F. W.; Tang, T.-H.; Tal, Y.; Biegler-König, F. W. *J. Am. Chem. Soc.* **1982**, *104*, 946.
(16) Alikhani, M. E. *Chem. Phys. Lett.* **1997**, *277*, 239.
(17) Dixon, R. E.; Streitwieser, A.; Laidig, K. E.; Bader, R. F. W.; Harder, S. *J. Phys. Chem.* **1993**, *97*, 3728.
(18) Glukhovtsev, M. N.; Pross, A.; Mcgrath, M. P.; Radom, L. *J. Chem. Phys.* **1995**, *103*, 1878.
(19) Ishida, G.; Morokuma, K.; Komornicki, A. *J. Chem. Phys.* **1977**, *66*, 2153.
(20) Frisch, M. J.; Trucks, G. W.; Schlegel, H. B.; Scuseria, G. E.; Robb, M. A.; Cheeseman, J. R.; Zakrzewski, V. G.; Montgomery, J. A., Jr.; Stratmann, R. E.; Burant, J. C.; Dapprich, S.; Millam, J. M.; Daniels, A. D.; Kudin, K. N.; Strain, M. C.; Farkas, O.; Tomasi, J.; Barone, V.; Cossi, M.; Cammi, R.; Mennucci, B.; Pomelli, C.; Adamo, C.; Clifford, S.; Ochterski, J.; Petersson, G. A.; Ayala, P. Y.; Cui, Q.; Morokuma, K.; Malick, D. K.; Rabuck, A. D.; Raghavachari, K.; Foresman, J. B.; Cioslowski, J.; Ortiz, J. V.; Stefanov, B. B.; Liu, G.; Liashenko, A.; Piskorz, P.; Komaromi, I.; Gomperts, R.; Martin, R. L.; Fox, D. J.; Keith, T.; Al-Laham, M. A.; Peng, C. Y.; Nanayakkara, A.; Gonzalez, C.; Challacombe, M.; Gill, P. M. W.; Johnson, B.; Chen, W.; Wong, M. W.; Andres, J. L.; Gonzalez, C.; Head-Gordon, M.; Replogle, E. S.; Pople, J. A. *Gaussian 98*; Gaussian, Inc.: Pittsburgh, PA, 1998.
(21) Biegler-König, F. *AIM 2000*, Version 1.0; University of Applied Science: Bielefeld, Germany, 2000.
(22) Zeng, Y. L.; Zheng, S. J.; Meng, L. P. *J. Phys. Chem. A* **2004**, *108*, 10527.
(23) Zeng, Y. L.; Zheng, S. J.; Meng, L. P. *Inorg. Chem.* **2004**, *43*, 5311.